SCIENCE CHINA
Earth Sciences

• RESEARCH PAPER •

doi: 10.1007/s11430-012-4522-0

A numerical study on matching relationships of gravity waves in nonlinear interactions

HUANG KaiMing[1,2,3*] ZHANG ShaoDong[1,2,3] & YI Fan[1,2,3]

[1] *School of Electronic Information, Wuhan University, Wuhan 430072, China;*
[2] *Key Laboratory of Geospace Environment and Geodesy, Ministry of Education, Wuhan 430072, China;*
[3] *State Observatory for Atmospheric Remote Sensing, Wuhan 430072, China*

Received April 13, 2012; accepted August 17, 2012

Applying a fully nonlinear numerical scheme with second-order temporal and spatial precision, nonlinear interactions of gravity waves are simulated and the matching relationships of the wavelengths and frequencies of the interacting waves are discussed. In resonant interactions, the wavelengths of the excited wave are in good agreement with the values derived from sum or difference resonant conditions, and the frequencies of the three waves also satisfy the matching condition. Since the interacting waves obey the resonant conditions, resonant interactions have a reversible feature that for a resonant wave triad, any two waves are selected to be the initial perturbations, and the third wave can then be excited through sum or difference resonant interaction. The numerical results for nonresonant triads show that in nonresonant interactions, the wave vectors tend to approximately match in a single direction, generally in the horizontal direction. The frequency of the excited wave is close to the matching value, and the degree of mismatching of frequencies may depend on the combined effect of both the wavenumber and frequency mismatches that should benefit energy exchange to the greatest extent. The matching and mismatching relationships in nonresonant interactions differ from the results of weak interaction theory that the wave vectors are required to satisfy the resonant matching condition but the frequencies are permitted to mismatch and oscillate with amplitude of half the mismatching frequency. Nonresonant excitation has an irreversible characteristic, which is different from what is found for the resonant interaction. For specified initial primary and secondary waves, it is difficult to predict the values of the mismatching wavenumber and frequency for the excited wave owing to the complexity.

gravity wave, nonlinear interaction, matching condition, detuning degree of interaction

Citation: Huang K M, Zhang S D, Yi F. A numerical study on matching relationships of gravity waves in nonlinear interactions. Sci China Earth Sci, 2012, doi: 10.1007/s11430-012-4522-0

Gravity waves play important roles in determining large-scale circulations and dynamics of the middle atmosphere because of their inherent ability to transport momentum from one level to another and deposit energy at the heights where the waves dissipate [1–4]. Many possible mechanisms of the generation, internal transfer and dissipation of gravity waves have been extensively explored in the past several decades. The most obvious sources of gravity waves in the lower atmosphere include flow over topography, convection, wind shear and adjustment of unbalanced flows in the vicinity of jet streams [5–7]. Additional sources, such as body forcing accompanying localized wave dissipation [8, 9], may be of significance in the middle and upper atmosphere [10]. On account of the diversity and variability of wave sources, gravity waves are generated on various spatial and temporal scales [11–14]. Since the amplitude of gravity waves increases exponentially with height, a nonlinear effect is one of the most significant features of gravity

*Corresponding author (email: hkm@whu.edu.cn)

waves in the middle and upper atmosphere. When gravity waves propagate in the middle and upper atmosphere, they represent a random encounter and superposition of many waves with different amplitudes, wave numbers and frequencies. At this time, there may also be redistribution of energy and momentum among different wave components with approximate conservation of total energy and momentum owing to nonlinear interactions, which may lead to the rapid relaxation of distorted spectra toward the universal form of gravity waves. Doppler spread theory presented by Hines [15] and Weinstock [16] employs statistical wave-wave interactions to account for the form of the saturated spectrum, and attributes the spectral energy transfer to Doppler spread. Weinstock [16] treated the effects of nonlinearity as a damping decrement in the dispersion relation of gravity waves and inferred an energy cascade to smaller wave scale. Hence, wave–wave interactions are regarded as an important mechanism in the energy exchanges and spectral evolution of gravity waves in the middle and upper atmosphere [15–18].

As a relatively mature theory, weak nonlinear interaction theory has been extensively applied to the phenomena of wave–wave interaction. Under the weak nonlinear approximation, the equations of motion are linearized, and then transformed into interaction equations. In this way, the amplitudes of the interacting waves are expressed as functions slowly varying in time, and the coupling coefficients can be written as expressions of the wave vectors and frequencies of the interacting waves. Hence, it is possible to discuss the feature of energy exchange among the wave triad. Employing weak interaction theory, many studies on the features and effects of resonant and nonresonant interactions among atmospheric gravity waves have been carried out [19–23]. Starting from a set of linearized resonant interaction equations, interaction rates for three resonant triads have been deduced [19]. Dong and Yeh [20] studied wave-wave interactions not confined to a resonance surface, and suggested that in the case of frequency mismatch, there might be nonresonant interaction with an amplitude threshold. Some characteristics of resonant and nonresonant interactions in a sheared, dissipative and rotating atmosphere have been acquired [22, 23]. Additionally, weak nonlinear approximation has been extended to investigate nonlinear interaction between planetary waves and inertial gravity waves in the atmosphere [24, 25]. These theoretical works revealed the essential property of nonlinear interaction of atmospheric waves in a weak nonlinear regime.

There has been a long debate over the validity range of weak interaction theory [10, 26, 27], which motivates the direct numerical simulations of wave-wave interactions. According to numerical studies, wave-wave interaction substantially reduces in momentum flux [27], and spatially localized interaction could transfer significant energy on a timescale of several periods of the primary wave [28]. Using the linearized resonant interaction equations, the temporal and spatial evolutions of gravity wave packets in resonant interactions have been investigated [29]. Starting from a set of nonlinear equations, gravity wave excitations due to resonant and nonresonant interactions have been clearly demonstrated in numerical experiments, showing that energy exchange in nonlinear interaction is irreversible rather than periodic as predicted by weak interaction theory [30–32]. Huang et al. [31] examined the effect of viscosity on nonresonant interaction. Their results showed that viscous dissipation mainly led to energy decay of the interacting waves, and the amplitude threshold for nonresonant interaction in the presence of viscosity predicted by weak interaction theory might be a rather loose restriction. Moreover, a detuning degree of interaction was introduced to determine whether there is effective energy exchange in nonlinear interactions [32].

In weak interaction theory, three resonant waves must satisfy both the wave vector and frequency matching conditions, which are expressed as

$$\vec{k_1} \pm \vec{k_2} = \vec{k_3}, \tag{1}$$

$$\omega_1 \pm \omega_2 = \omega_3\,, \tag{2}$$

where the subscripts j = 1, 2 and 3 denote the interacting waves, which are named the primary, secondary and excited waves; and $\vec{k}$ and ω are the wave vector and frequency. The wave vector and frequency for each wave obey the dispersion relation $\omega_j = \Omega(\vec{k}_j)$, which can be written as

$$\frac{{k_x}^2}{(\omega^2 - {\omega_\mathrm{a}}^2)/(\omega^2 - N^2)} + \frac{{k_z}^2}{(1 - {\omega_\mathrm{a}}^2/\omega^2)} = \frac{\omega^2}{{v_\mathrm{a}}^2}, \tag{3}$$

where k_x and k_z are the horizontal and vertical components of the wave vectors, respectively; N is the buoyancy frequency; v_a is the acoustic speed; and ω_a is the acoustic-cutoff frequency. These two types of interactions presented in the resonant conditions of eqs. (1) and (2) are referred to as sum and difference resonant interactions, respectively.

In resonant interaction, for two specified initial waves, the wavelengths and frequencies of the excited waves can be derived from the resonant conditions. It should be noted that because resonant interaction is restricted by the severe matching conditions, nonresonant interaction may occur more frequently than resonant interaction. However, for nonresonant interaction, owing to approximations and the complicated eigenvalue and eigenvector obtained from the linearized interaction equations, weak interaction theory may give unintelligible results. For example, three nonresonant waves are required to satisfy the wavenumber matching condition, and only their frequencies are permitted to mismatch; moreover, the frequencies of both the excited and secondary waves oscillate with amplitude of half the mismatching frequency [20, 22, 23]. This means that the excited and secondary waves do not obey the dispersion relation of gravity waves in interaction. Fritts et al. [22] relaxed the limit of the wavenumber matching condition, and proposed that there might be a mismatch of wavenumbers as well as frequencies in nonresonant interaction. Nevertheless, in this case, it is difficult to obtain not only the mismatching degrees of wavenumbers and frequencies but also the expressions of the interaction coefficients. Hence, there remains much to be done in quantitative studies on the matching relationships of the wavelengths and frequencies of nonresonant waves. Previous numerical studies paid more attention to energy exchange in a certain sum or difference interaction. In this paper, we focus on the relation of three waves in resonant and nonresonant excitations by investigating sum and difference nonlinear interactions of wave triads, and explore the match and mismatch among the interacting waves, which is helpful in understanding the nonlinearity of gravity waves.

1 Numerical model

1.1 Governing equations and numerical scheme

The simulations adopt a set of primitive hydrodynamic equations for an adiabatic, inviscid and two-dimensional compressible atmosphere, which can be written as

$$\begin{cases} \dfrac{\partial \rho}{\partial t}+u\dfrac{\partial \rho}{\partial x}+w\dfrac{\partial \rho}{\partial z}+\rho\dfrac{\partial u}{\partial x}+\rho\dfrac{\partial w}{\partial z}=0, \\ \dfrac{\partial u}{\partial t}+u\dfrac{\partial u}{\partial x}+w\dfrac{\partial u}{\partial z}+\dfrac{RT}{\rho}\dfrac{\partial \rho}{\partial x}+R\dfrac{\partial T}{\partial x}=0, \\ \dfrac{\partial w}{\partial t}+u\dfrac{\partial w}{\partial x}+w\dfrac{\partial w}{\partial z}+\dfrac{RT}{\rho}\dfrac{\partial \rho}{\partial z}+R\dfrac{\partial T}{\partial z}+g=0, \\ \dfrac{\partial T}{\partial t}+u\dfrac{\partial T}{\partial x}+w\dfrac{\partial T}{\partial z}+T(\gamma-1)\left(\dfrac{\partial u}{\partial x}+\dfrac{\partial w}{\partial z}\right)=0, \end{cases} \tag{4}$$

where x and z are the horizontal and vertical (positive upward) coordinates, respectively; u and w are the horizontal and vertical components of the total wind field, respectively; ρ and T are the density and temperature, respectively; g is the acceleration due to gravity; R=287 J kg^{-1} K^{-1} is the special gas constant for air; and $\gamma=c_p/c_v$ (c_p=1005 J kg^{-1} K^{-1} and c_v=718 J kg^{-1} K^{-1} are specific heats at constant pressure and volume, respectively).

Usually, the propagation of gravity waves in the atmosphere is a long-lasting process. To precisely simulate the propagation and interaction of gravity waves, a numerical scheme should be of high accuracy and fine stability. Here, a composite difference scheme with second-order temporal and spatial precision, which was described in detail by Huang et al. [31], is applied to discretizing the equations (4), and a corresponding three-dimensional model is extended to investigate the propagation characteristics of gravity waves [33].

To avoid the boundary reflection, the lateral boundaries are set to be periodic, and projected characteristic line boundaries are employed at the top and bottom boundaries [34]. In view of an explicit scheme used for the projected characteristic line boundaries, the time step should be restricted by the Courant condition:

$$\Delta t<\Delta t_{\mathrm{c}}=\frac{1}{(v_{\mathrm{a}}+v)\left(\dfrac{1}{\Delta x^2}+\dfrac{1}{\Delta z^2}\right)^{1/2}}, \tag{5}$$

where the acoustic speed $v_{\mathrm{a}}=\sqrt{\gamma RT}$, and $v=\sqrt{u^2+w^2}$. In this paper, we take $\Delta t=0.5\Delta t_{\mathrm{c}}$.

1.2 Initial background and perturbation

To investigate the matching relations of the wavenumbers and frequencies of the interacting gravity waves, we avoid the influences of background wind and inhomogeneous temperature fields by assuming that the initial background atmosphere is windless and isothermal and is in hydrostatic equilibrium with initial constant temperature of T_0=290 K and initial density profile of $\rho_0=\rho_c\mathrm{e}^{-gz/RT_0}$, where ρ_c = 1.2 kg m^{-3} is the density at ground level.

In the initial background atmosphere, we introduce two discrete gravity wave packets as the initial wave perturbations, of which the horizontal velocity disturbances have the Gaussian form

$$u_j'(x,z,t)\big|_{t=0}=u_{cj}\mathrm{e}^{-\frac{(x-x_{cj})^2}{2\delta_{xj}^2}}\mathrm{e}^{-\frac{(z-z_{cj})^2}{2\delta_{zj}^2}}\sin[k_{xj}(x-x_{cj})+k_{zj}(z-z_{cj})-\omega t],$$

where u_{cj} (j=1 and 2) is the maximum horizontal wind amplitude; x_{cj} and z_{cj} are the initial geometric center positions of the wave packets in x and z directions, respectively; and σ_{xj} and σ_{zj} represent the half–widths of the wave packets in x and z directions, which are chosen to be $\sigma_{xj}=\sigma_{zj}$ and $\sigma_{zj}=\lambda_{zj}$, where λ_{xj} and λ_{zj} are the horizontal and vertical wavelengths of the interacting waves, respectively. The other initial perturbation quantities (w_j', ρ_j', T_j') are derived from the polarization equations of gravity waves.

2 Matching among the resonant triad

Observations show that the horizontal wavelengths of atmospheric gravity waves range from several ten to several hundred kilometers, the vertical wavelengths from several to more than ten kilometers, and the intrinsic frequencies from the inertial frequency to buoyancy frequency [11–14, 35]. In case 1, we choose the horizontal and vertical wavelengths for the primary wave to be 50 and 5 km, of which the frequency is derived as 18.05×10^{-4} rad s^{-1}, from the dispersion relation of eq. (3). For resonant interaction, the secondary wave should be selected from the resonant curve of the primary wave, which is determined by the resonant conditions of eqs. (1) and (2) and the dispersion relation of eq. (3). Hence, the wavelengths of the secondary wave are chosen to be 129.67 and –2.3 km in the horizontal and vertical directions, respectively, where the negative sign in front of the vertical wavelength denotes downward phase progression but upward wave energy propagation, and the corresponding frequency is 3.22×10^{-4} rad s^{-1}. According to eqs. (1)–(3), the excited wave would have horizontal and vertical wavelengths of 36.08 and –4.26 km, and frequency of 21.27×10^{-4} rad s^{-1}, if there is resonant interaction. In the atmosphere, when the amplitudes of upward propagating gravity waves reach their instability thresholds, wave breaking may occur, and the body force due to local breaking of waves tends to create high-frequency gravity waves with large vertical group velocity [8, 9]. Besides this, the upward propagating high-frequency gravity waves are likely to experience reflection in the shear wind and temperature gradient of the middle and upper atmosphere, and turn to propagate downwards [36]. Observations from radiosondes show that the fraction of downward propagating gravity waves is about 20%–30% in the stratosphere [11, 12, 14]. In case 1, the primary wave is chosen to be a downward propagating high-frequency perturbation with large vertical scale. Hereby, it should be pointed out that all wavelengths and frequencies of the wave triad presented here are typical observational values in the atmosphere, and the upward and downward propagations of the wave triad are also consistent with observations [11, 13, 35]. Table 1 lists the wavelengths and frequencies of these resonant three waves. In the first case group (cases 1–3), besides waves 1 and 2 being selected as the initial wave perturbations in case 1, waves 2 and 3 and waves 1 and 3 are selected as the initial wave perturbations in cases 2 and 3, respectively.

According to the wavenumbers and frequencies of this wave triad listed Table 1, one can easily verify that the sum resonant excitation may occur in case 1 because of $\vec{k}_1+\vec{k}_2=\vec{k}_3$ and $\omega_1+\omega_2=\omega_3$, while difference resonant excitations probably arise in cases 2 and 3 because of $\vec{k}_3-\vec{k}_2=\vec{k}_1$ and $\omega_3-\omega_2=\omega_1$ in case 2, and $\vec{k}_3-\vec{k}_1=\vec{k}_2$ and $\omega_3-\omega_1=\omega_2$ in case 3. When waves 1–3 are regarded as the initial wave perturbations, their amplitudes and center positions are also listed in Table 1. In the numerical computation, on the basis of the scale of waves 1–3 in this case group, the spatial grid sizes in the horizontal and vertical directions are set to be $\Delta x=3.6$ km and $\Delta z=0.23$ km, and the computational domains are chosen to be $0\leqslant x\leqslant 2376$ km and $0\leqslant z\leqslant 184$ km in the horizontal and vertical directions, respectively.

Figure 1 shows new wave excitation through nonlinear interaction using the square-root density-weighted horizontal velocity disturbances in cases 1–3, which are calculated from the expression of $u''(z)=[\rho_0(z)/\rho_{0r}]^{1/2}u'(z)$, where ρ_{0r} is the background density at a reference level of z=60 km. At the start time, there are two separate initial waves at different heights. At t= 5 h, new waves are excited through nonlinear interactions, and after propagation and interaction for 9 h, these interacting waves are almost apart from each other in each case.

To investigate the matching relationships of the wavenumbers and frequencies among the interacting waves, the wavenumber spectra of three waves are obtained by making a discrete Fourier transformation of the square-root density-weighted horizontal velocity disturbances over the whole computational domain. The calculated wavenumber spectra are normalized by the maximum spectral magnitude at the start time. Figure 2 shows the normalized wavenumber spectra of the interacting waves at t= 0 and 9 h for cases 1–3. According to the spectrum of the excited wave after 9 hours, we calculate the dominant wavelengths of the excited waves. In cases 1–3, the horizontal and vertical wavelengths of the excited waves are 36.0 and –4.28 km, 50.55 and 4.97 km, and 125.05 and –2.30 km, respectively, which are in agreement with matching wavelengths listed in Table 1. The tiny distinctions between the calculated and matching wavelengths are due to the limited spectral resolution in the numerical computation. The frequencies of the excited waves are calculated to be 21.42×10^{-4}, 17.75×10^{-4} and 3.34×10^{-4} rad s^{-1} in cases 1–3, and the deviations from the matching frequencies listed in Table 1 are small values of 0.7%, 1.7% and 3.8%, resulting from the wavelength errors due to the spectral resolution. Figure 2 shows that the dominant wavelengths of the primary and secondary waves remain unchanged in the interactions in each case. This means that in the sum and difference resonant interactions, both the wavelengths and frequencies of the interacting waves satisfy the resonant matching conditions, as predicted by weak interaction theory. Since the resonant conditions are satisfied, for a resonant wave triad, any two waves are chosen to be the initial wave perturbations, and the third wave is then

Table 1 Initial parameters of waves 1–3 regarded as initial perturbations in cases 1–3

	λ_x (km)	λ_z (km)	k_x (10^{-4} rad m^{-1})	k_z (10^{-3} rad m^{-1})	ω (10^{-4} rad s^{-1})	u_c (m s^{-1})	x_c (km)	z_c (km)
Wave 1	50	5.0	1.26	1.26	18.05	5.0	500	80
Wave 2	129.67	-2.3	0.48	–2.73	3.22	1.0	600	60
Wave 3	36.08	-4.26	1.74	–1.47	21.27	0.4	530	43

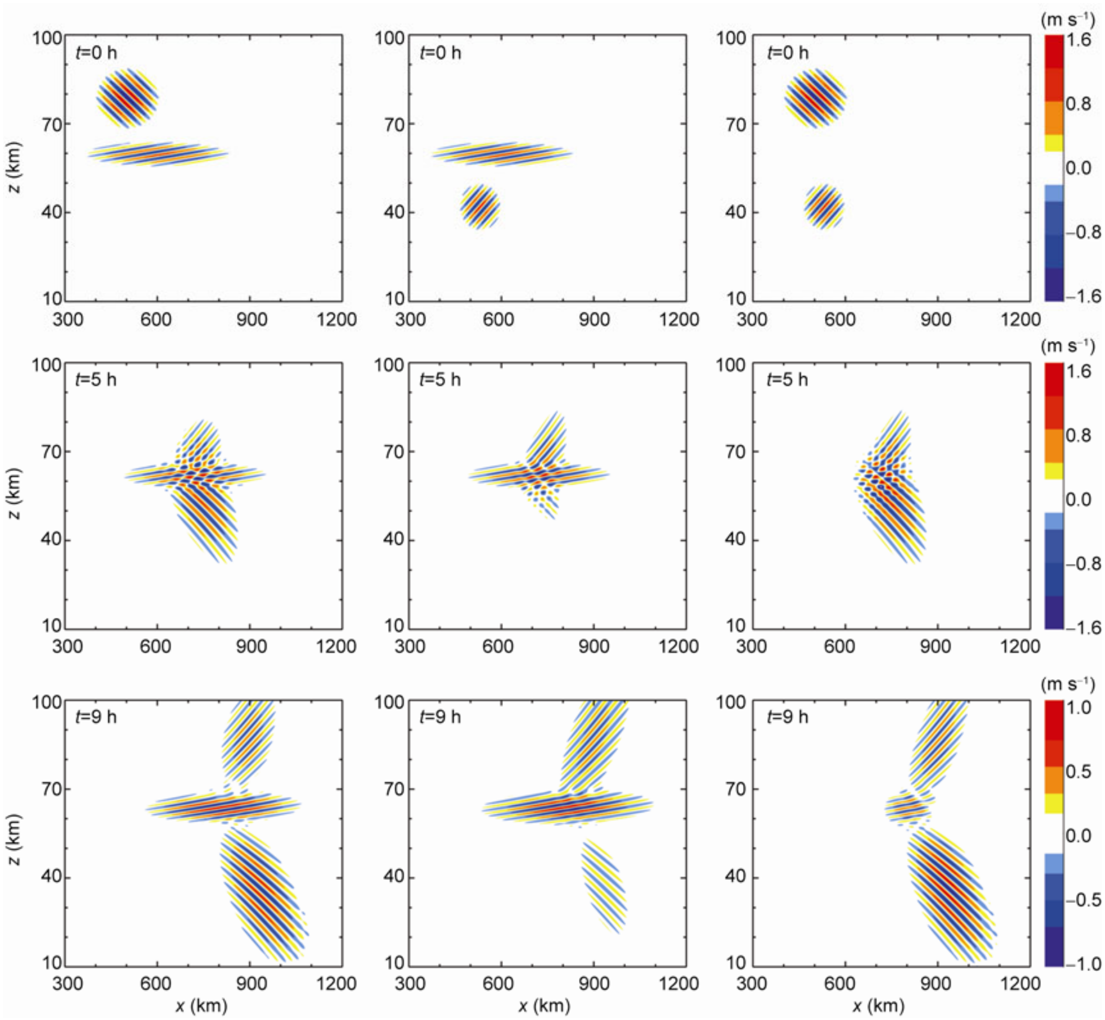

Figure 1 Sum and difference resonant interactions. The first, second and third columns correspond to cases 1–3, respectively.

excited through the sum or difference resonant interaction, as shown in Figures 1. In other words, the resonant interaction has a reversible excitation characteristic.

3 Mismatch in nonresonant interaction

3.1 Nonresonant case

For the second case group (cases 4–6), we first simulate case 4. In case 4, downward propagating wave 1 and upward propagating wave 2 are chosen as the initial waves; their parameters are listed in Table 2. Here, the possible interaction between these two waves is discussed in brief. Supposing an excited wave obeys the sum matching condition for wavenumbers, its wavelengths should equal the matching wavelengths (L_x and L_z), i.e., $\lambda_{x3}=L_{sx}=$ 35.29 km and $\lambda_{z3}=L_{sz}=-3.33$ km. Its frequency is then derived from the dispersion relation as 17.06×10^{-4} rad s^{-1}, which is smaller than the sum (21.08×10^{-4} rad s^{-1}) of the frequencies of waves 1 and 2. This means that the sum resonant interaction does not take place because the sum matching condition of frequencies cannot be satisfied. On the other hand, if an excited wave meets the difference matching condition of wavenumbers, its wavelengths are calculated to be $\lambda_{x3}=L_{dx}=$ 85.71 km and $\lambda_{z3}=L_{dz}=1.43$ km; thus, its frequency is 3.03×10^{-4} rad s^{-1}. We can take notice of this frequency much less than the difference (15.02×10^{-4} rad s^{-1}) of the frequencies of waves 1 and 2. Hence, the difference matching condition for frequencies is not satisfied either, which indicates that there is no difference resonant interaction. Since neither a sum nor difference resonant interaction can occur, a new wave would be excited only through nonresonant interaction if it arose. Huang et al. [32] introduced a detuning degree of interaction, $\delta=\left|\dfrac{\Omega(\vec{k}_1)\pm\Omega(\vec{k}_2)-\Omega(\vec{k}_1\pm\vec{k}_2)}{\Omega(\vec{k}_1\pm\vec{k}_2)}\right|$, which may be applied to determining whether there is an effective energy exchange in the nonlinear interaction of gravity waves. According to the wavenumbers of waves 1 and 2 listed in Table 2, the detuning degrees of sum and differ-

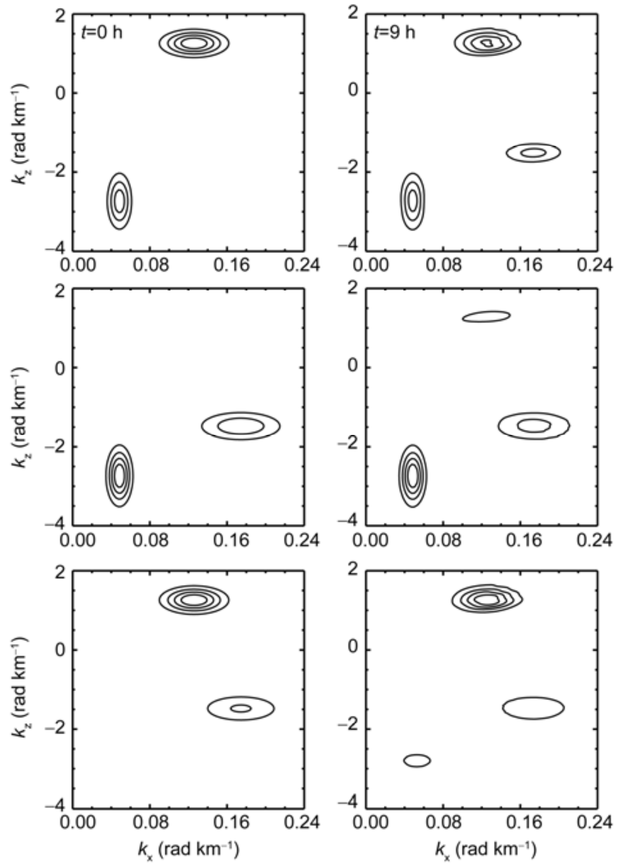

Figure 2 Normalized wave number spectra in cases 1–3. The contour values are 0.2, 0.4, 0.6 and 0.8. The first, second and third rows correspond to cases 1–3, respectively.

ence interactions are calculated to be δ_s=0.23 and δ_d=3.97, respectively. Such a large detuning degree of the difference interaction (δ_d=3.97) implies that there is no significant energy transfer in the difference nonresonant interaction. However, considering a small detuning degree of the sum interaction (δ_s=0.23), one expects that a new wave may be excited through the sum nonresonant interaction. Furthermore, we can distinguish a new wave excited through the sum nonresonant interaction from one excited through the difference nonresonant interaction only by its upward propagation because the new wave would propagate downwards if the difference nonresonant interaction between waves 1 and 2 listed in Table 2 excited a third wave. In addition, in the numerical computation, considering the spatial scale of the interacting waves, the grid sizes are adjusted to be Δx=3.5 km and Δz=0.2 km, and the hori- zontal and vertical domains are altered to be 0 km$\leqslant x \leqslant$2520 km and 0 km$\leqslant z \leqslant$172 km, respectively.

Figure 3 shows the nonlinear interaction process using square-root density-weighted horizontal velocity disturbances. As we expected, a new wave (wave 3) is excited through the sum nonresonant interaction because of its upward propagation direction. Figure 4 shows the normalized wavenumber spectra of the interacting waves. In Figure 4, the two values in brackets denote the dominant horizontal and vertical wavelengths of the excited wave derived from the corresponding wavenumbers at the peak. From 7 to 10 h, the wavelengths of the excited wave maintain the constant values of 35.49 and –4.0 km in the horizontal and vertical directions, respectively, and the frequency is calculated to be 20.32×10^{-4} rad s^{-1}, which also remains unchanged in the interaction. It is interesting that the horizontal wavelength of wave 3 (λ_{x3}= 35.49 km) is consistent with its matching value (L_{sx}= 35.29 km), while its vertical wavelength (λ_{z3}= –4.0 km) is obviously greater than its matching value (L_{sz}= –3.33 km). In the whole propagation and interaction process, as shown in Figure 4, the dominant wavelengths of waves 1 and 2 in both the horizontal and vertical directions remain invariable; thus, the frequencies are fixed at 18.05×10^{-4} and 3.03×10^{-4} rad s^{-1} as listed in Table 2. The frequency (20.32×10^{-4} rad s^{-1}) of wave 3 is slightly lower than the sum (21.08×10^{-4} rad s^{-1}) of the frequencies of waves 1 and 2. Therefore, this nonresonant case shows that the frequency of the excited wave approaches the matching value, and the wave vectors of waves 1–3 seem to match in the horizontal direction, but not in the vertical direction.

3.2 Nonresonant triad

In case 4, for given wave 1 (λ_{x1}= 50 km and λ_{z1}= 5.0 km) and wave 2 (λ_{x2}= 120 km and λ_{z1}= –2.0 km), wave 3 with λ_{x3}= 35.49 km and λ_{z3}= –4.0 km is excited through the sum nonresonant interaction; thus, waves 1–3 make up a nonresonant triad. In cases 5 and 6, we choose waves 2 and 3 and waves 1 and 3 to be the initial wave perturbations, respectively. The initial parameters of wave 3, as the initial wave in cases 5 and 6, are also listed in Table 2. This indicates that when waves 1–3 are selected to be the initial perturbations, their initial parameters are identical in different cases. In cases 5 and 6, the detuning degrees of sum interaction are calculated to be δ_s= 1.64 and 0.70, respectively, while the detuning degrees of difference interaction are δ_d= 0.20 and 0.31, respectively. Therefore, the difference nonresonant interaction may arise in both cases 5 and 6 owing

Table 2 Initial parameters of waves 1–3 regarded as initial perturbations in cases 4–6

	λ_x (km)	λ_z (km)	k_x (10^{-4} rad m^{-1})	k_z (10^{-3} rad m^{-1})	ω (10^{-4} rad s^{-1})	u_c (m s^{-1})	x_c (km)	z_c (km)
Wave 1	50	5.0	1.26	1.26	18.05	5.0	488	80
Wave 2	120	–2.0	0.52	–3.14	3.03	1.0	600	60
Wave 3	35.49	–4.0	1.77	–1.57	20.32	0.4	526	44.4

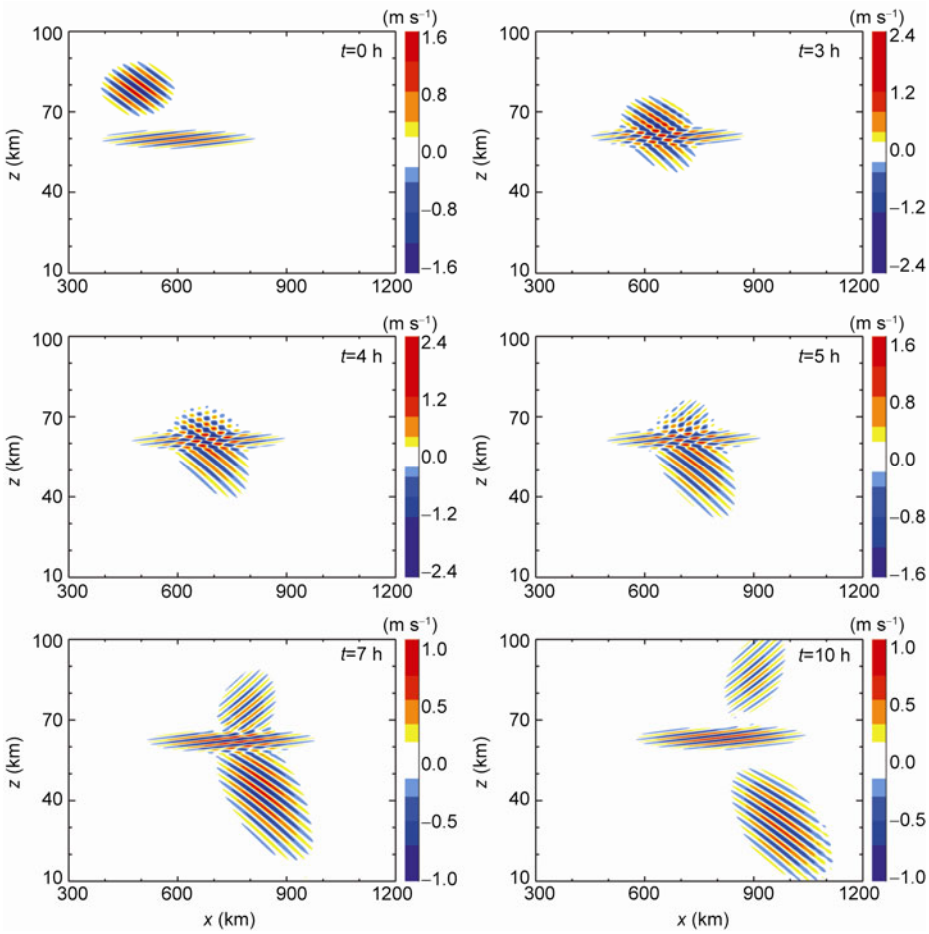

Figure 3 Sum nonresonant interaction in case 4.

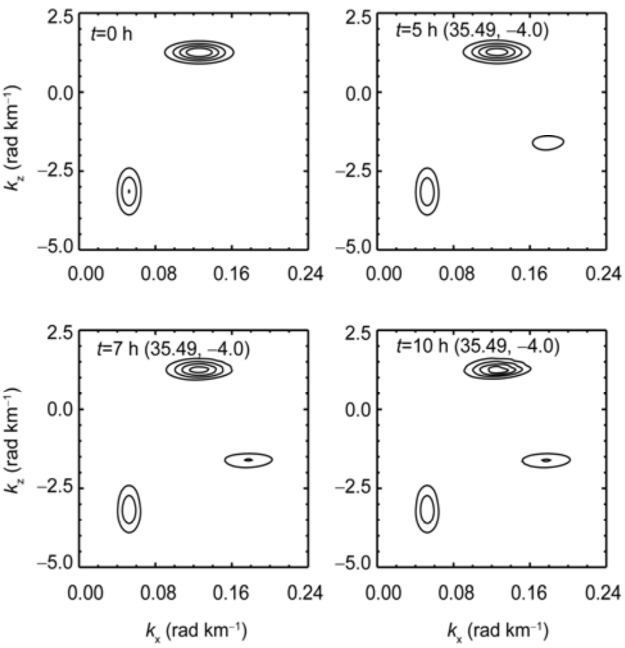

Figure 4 Normalized wave number spectra in case 4. The contour values are 0.2, 04, 0.6 and 0.8. The two values in each set of brackets denote the dominant horizontal and vertical wavelengths of the excited wave in unit of kilometers.

to the detuning degrees of the difference interaction being much less than the detuning degrees of the sum interaction. The nonlinear excitations for cases 5 and 6 are shown in Figure 5. The normalized wavenumber spectra of the interacting waves at t= 0 and 10 h are shown in Figure 6. Similar to cases 1–4, after 10 h, the wavelengths of the primary and secondary waves remain similar to their initial values. In case 5, the excited wave has horizontal and vertical wavelengths of 50.40 and 4.41 km, and its frequency is derived from the dispersion relation as 15.81×10^{-4} rad s^{-1}, which is lower than the value (17.29×10^{-4} rad s^{-1}) of $\omega_3-\omega_2$. In case 6, the wavelengths of the excited wave are 100.8 and –2.21 km in the horizontal and vertical directions, and its frequency of 3.98×10^{-4} rad s^{-1} is larger than the value (2.27×10^{-4} rad s^{-1}) of $\omega_3-\omega_1$. The excited waves in cases 5 and 6 are different from wave 1 and wave 2; thus, we refer to these new waves as waves 4 and 5 in cases 5 and 6, respectively. This indicates that for a nonresonant wave triad, once any of the two initial waves is replaced with the third wave, the anew excited wave is not the replaced wave any more, which differs from the reversible characteristic in resonant interaction.

Figure 7 shows the wave vectors of waves 1–5 and the matching wave vectors in cases 4–6. In cases 4 and 5, the

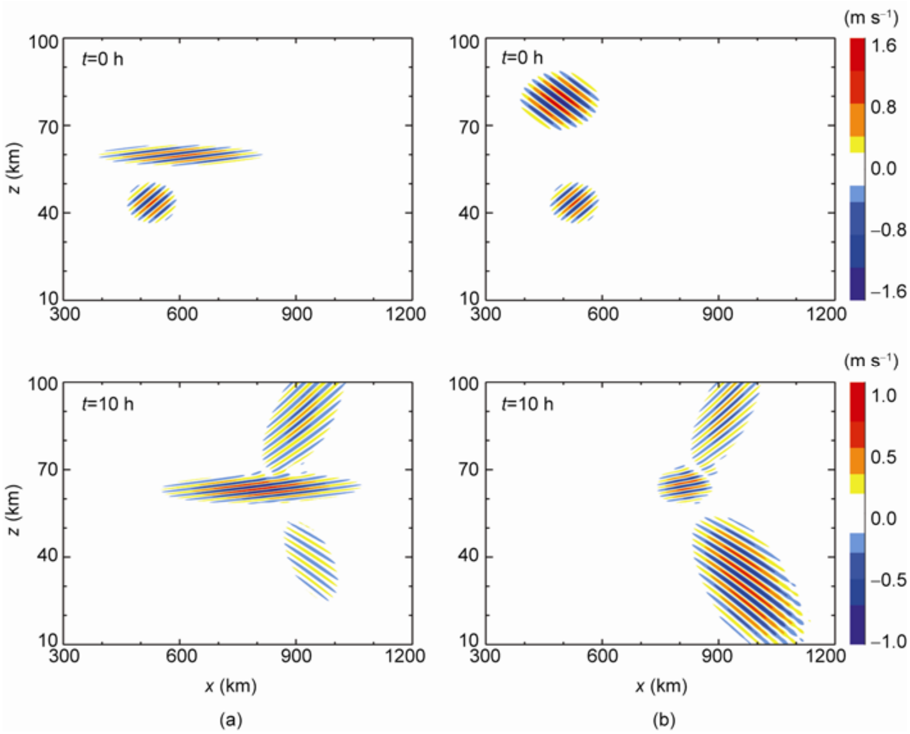

Figure 5 Difference nonresonant excitations for cases 5 (a) and 6 (b).

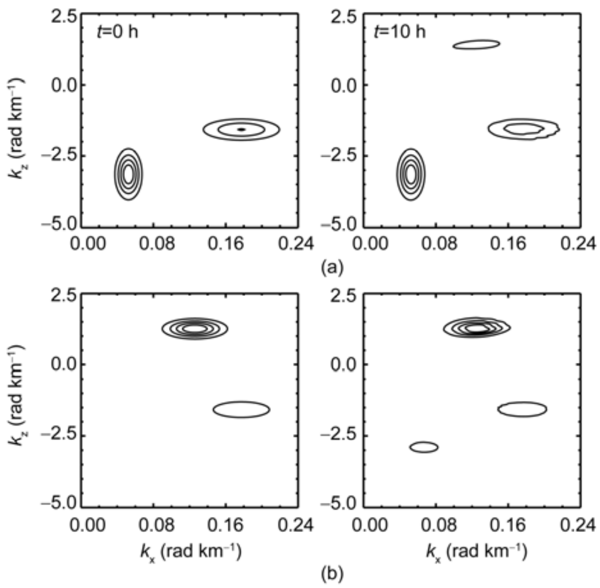

Figure 6 Normalized wave number spectra for cases 5 (a) and 6 (b). The values of contours are 0.2, 0.4, 0.6 and 0.8.

horizontal wavenumbers of the excited waves (waves 3 and 4) almost equal the matching values, while in case 6, the excited wave (wave 5) has a vertical wavenumber close to its matching value. Therefore, in the nonresonant interaction, although the three wave vectors mismatch, their horizontal components approximately meet the matching condition, or their vertical components tend to match.

3.3 More nonresonant triads

Several nonresonant wave triads are investigated to further reveal the general characteristics of the nonresonant excitations. For the third case group (cases 7–9), firstly, we numerically study case 7. In case 7, the initial parameters of initial waves 1 and 2 are listed in Table 3. The detuning degrees of sum and difference interactions are δ_s=0.28 and δ_d=3.43, which implies that a new wave will be excited through the sum nonresonant interaction. The sum matching wavelengths are calculated to be L_{sx}=38.10 km and L_{sz}=–3.33 km from the sum matching condition of the wavenumber. According to the wavenumber spectra of the interacting waves at t=10 h, the excited wave (wave 3) has wavelengths of λ_{x3}=38.18 km and λ_{z3}=–4.0 km, and the frequency of 18.91×10^{-4} rad s^{-1} is lower than the sum (20.32×10^{-4} rad s^{-1}) of the frequencies of waves 1 and 2. Hereby, waves 1–3 constitute a nonresonant triad. Next, waves 2 and 3 and waves 1 and 3 are regarded as the initial waves to simulate cases 8 and 9, respectively. When wave 3 is selected to be the initial wave perturbations, its parameters are also presented in Table 3. In case 8, the new wave (wave 4) is a downward propagating wave with λ_{x4}=50.04 km and λ_{z4}=–4.30 km. Thus, its frequency is 15.53×10^{-4} rad s^{-1}, which is a bit lower than the difference (16.64×10^{-4} rad s^{-1}) in frequencies of waves 2 and 3. In case 9, the wavelengths of the excited wave (wave 5) are λ_{x5}=126.0 km and λ_{z5}=–2.21 km, and wave 5 has frequency of 3.18×10^{-4} rad s^{-1}, which is higher than the difference (0.86×10^{-4} rad s^{-1})

in the frequencies of waves 1 and 3. We then consider the fourth case group (cases 10–12). In the fourth group of cases, the two initial waves are selected to be waves 1 and 2, waves 2 and 3, and waves 1 and 3 in cases 10–12, respectively. Initial parameters of waves 1–3 are listed in Table 4. In case 10, the sum matching wavelengths are L_{sx}= 35.29 km and L_{sz}= –5.0 km; however, the excited wave has wavelengths of λ_x= 35.49 km and λ_z= –4.3 km, and frequency of 21.82×10^{-4} rad s^{-1}, which are consistent with those of wave 3 listed in Table 4. It is obvious that these three waves do not obey the resonant conditions; thus, waves 1–3 presented in Table 4 also constitute a nonresonant triad. At t=10 h, the spatial scales of excited waves (waves 4 and 5) are λ_{x4}=50.40 km and λ_{z4}=5.12 km in case 11, and λ_{x5}=100.8 km and λ_{z5}=–2.29 km in case 12, and the corresponding frequencies of waves 4 and 5 are 18.33×10^{-4} and 4.12×10^{-4} rad s^{-1}. It is an interesting phenomenon that the frequencies of new waves 3–5 are rather close to the matching values (21.83×10^{-4}, 18.04×10^{-4} and 3.77×10^{-4} rad s^{-1}) of ω_1–ω_3 in case 10, ω_3–ω_2 in case 11, and ω_3–ω_1 in case 12, respectively.

Figures 8 and 9 display the relationship among the wave vectors of the interacting waves and the matching wave vectors in cases 7–9 and cases 10–12, respectively. Similar to Figure 7, Figures 8 and 9 show two common features of the nonresonant interactions. The first is the characteristic

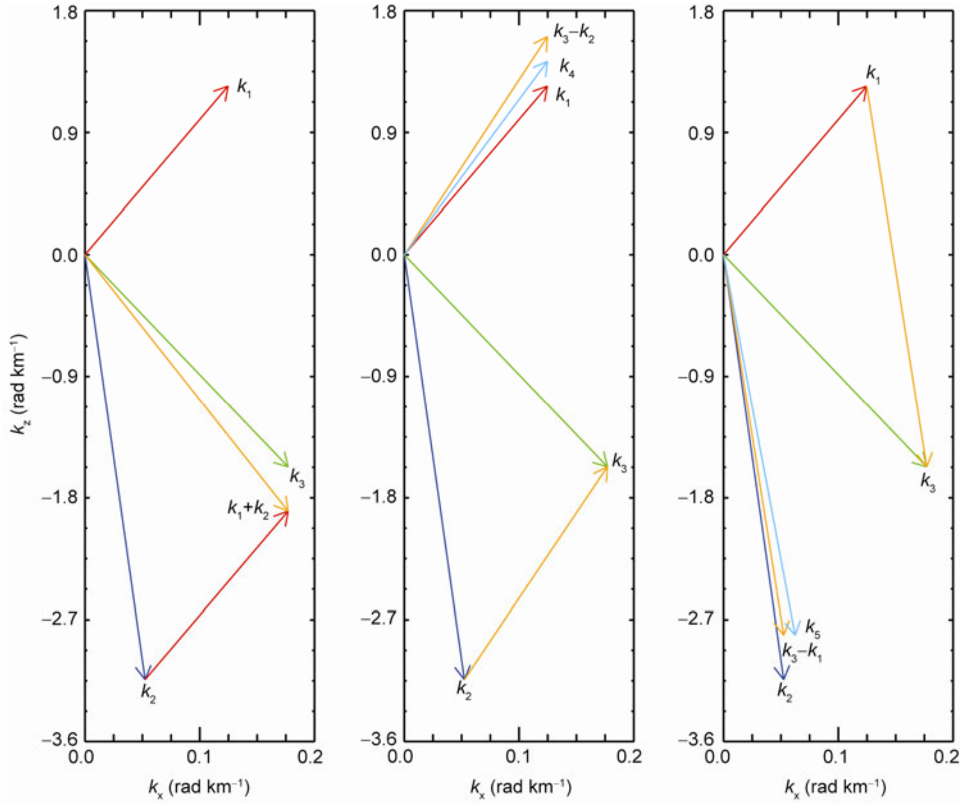

Figure 7 Wave vectors of waves 1–5 and matching wave vectors in cases 4–6.

Table 3 Initial parameters of waves 1–3 regarded as initial perturbations in cases 7–9

	λ_x (km)	λ_z (km)	k_x (10^{-4} rad m^{-1})	k_z (10^{-3} rad m^{-1})	ω (10^{-4} rad s^{-1})	u_c (m s^{-1})	x_c (km)	z_c (km)
Wave 1	50	5.0	1.26	1.26	18.05	5.0	487	80
Wave 2	160	–2.0	0.39	–3.14	2.27	1.0	600	60
Wave 3	38.18	–4.0	1.65	–1.57	18.91	0.4	520	44

Table 4 Initial parameters of waves 1–3 regarded as initial perturbations in cases 10–12

	λ_x (km)	λ_z (km)	k_x (10^{-4} rad m^{-1})	k_z (10^{-3} rad m^{-1})	ω (10^{-4} rad s^{-1})	u_c (m s^{-1})	x_c (km)	z_c (km)
Wave 1	50	5.0	1.26	1.26	18.05	5.0	511	80
Wave 2	120	–2.5	0.52	–2.51	3.78	1.0	600	60
Wave 3	35.49	–4.30	1.77	–1.46	21.82	0.4	536	43

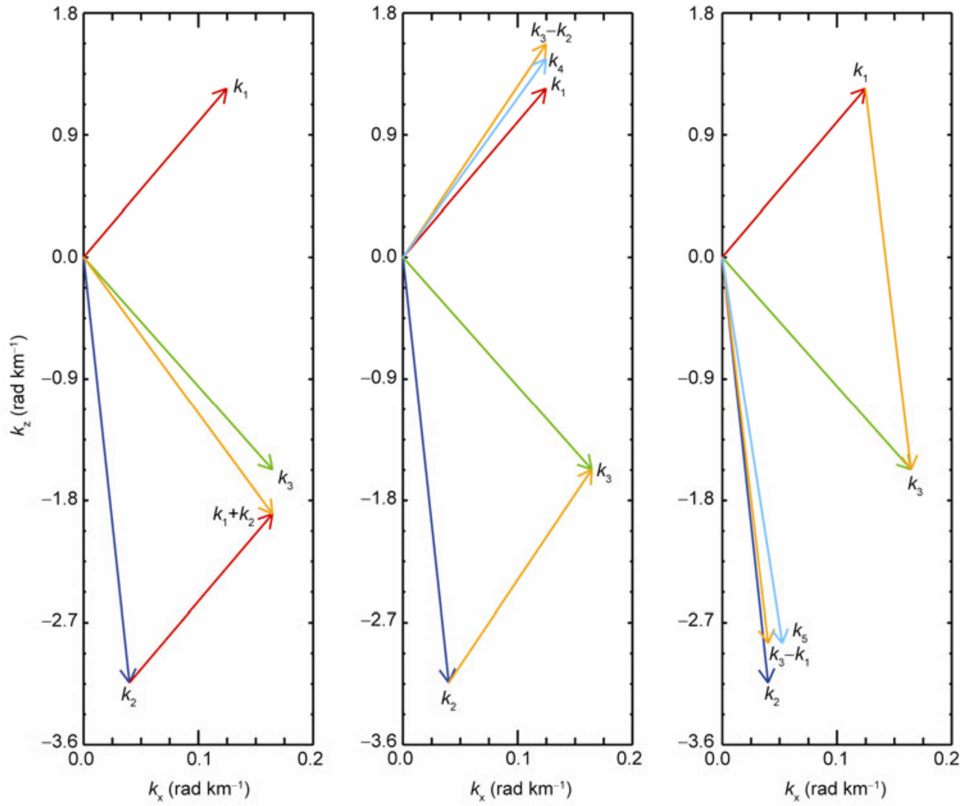

Figure 8 Wave vectors of waves 1–5 and matching wave vectors in cases 7–9.

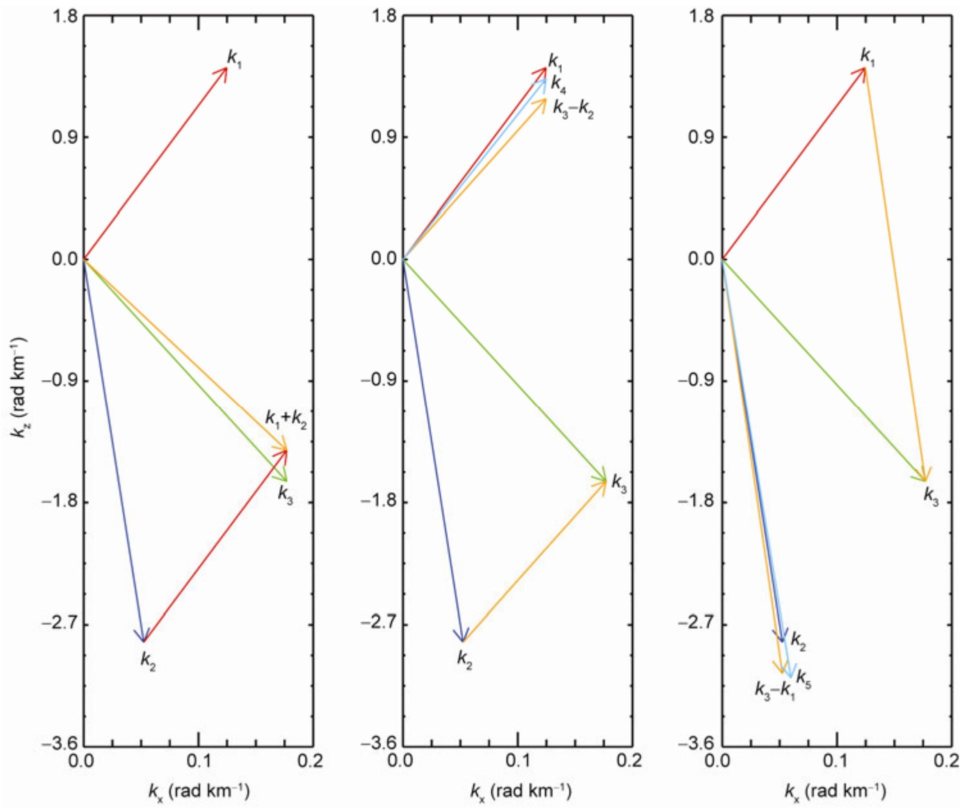

Figure 9 Wave vectors of waves 1–5 and matching wave vectors in cases 10–12.

of irreversible excitation. For a nonresonant triad, if any of the two initial waves is substituted by the third wave, the anew excited wave is different from the substituted wave. The second is the approximate matching of wave vectors in a single direction, especially in the horizontal direction, such as cases 4 and 5, cases 7 and 8, and cases 10 and 11. In these cases, the excited wave, with large vertical scale, is generated through the interaction of the primary wave with a low-frequency secondary wave. We can make a conjecture about the approximate matching of horizontal wavenumbers. If both the horizontal and vertical components of the wave vectors meet the matching conditions in the nonresonant interaction, the frequencies of the three waves may mismatch too much; thus, this situation does not benefit the energy exchange to the greatest extent. To moderately diminish the mismatching degree of frequencies, the vertical wavenumber of the excited wave may be moderately adjusted because the frequency of the gravity wave is more sensitive to the variation in the vertical number than in the horizontal number owing to the vertical wavenumber generally being 1–2 orders of magnitude larger than the horizontal wavenumber. In this case, the horizontal components of wave vectors may approximately remain matched. For instance, in case 4, if $\lambda_{x3}=L_{sx}=35.29$ km and $\lambda_{z3}=L_{sz}=-3.33$ km, the frequency of 17.06×10^{-4} rad s^{-1} for the new wave is much lower than the value (21.08×10^{-4} rad s^{-1}) of $\omega_1+\omega_2$; thus, this large frequency mismatch may prevent the exchange of wave energy as much as possible. The numerical results show that the frequency (20.32×10^{-4} rad s^{-1}) of the excited wave is close to the matching value (21.08×10^{-4} rad s^{-1}) owing to its vertical wavelength adjustment. In this instance, a considerable energy exchange arises. In cases 6, 9 and 12, the new wave with small vertical wavelength is excited through the interaction between two high–frequency waves. Since the vertical wavelength of the excited wave is rather small, it is possible that both the horizontal and vertical wavelengths of the excited wave moderately adjust, and even that the wavelength has a more obvious adjustment in the horizontal direction than in the vertical direction. With the moderate adjustment of wavenumbers, the degree of mismatching in frequencies can reduce, and may even approaches zero, which means the approximate matching of the frequencies of the three waves, such as in the fourth case group. Hence, the matching relationships of wavenumbers and frequencies in the nonresonant interaction are complex, and are different from the results obtained with weak interaction theory [21, 23, 25].

4 Summary

The matching relationships among gravity waves in resonant and nonresonant interactions were investigated in numerical experiments. In resonant interactions, the wavelengths of the excited wave are in good agreement with the values derived from the resonant conditions, and the frequencies of the three waves also meet the matching condition, such as in the first case group. Because the resonant conditions are satisfied, the resonant excitations have a reversible characteristic that for a resonant wave triad, any two waves are chosen to be the initial wave perturbations, and the third wave can then be excited through the sum or difference resonant interaction. However, relative to resonant interactions, nonresonant interactions have complicated matching relations. In nonresonant interactions, the wave vectors tend to approximately match in a single direction, generally in the horizontal direction. The frequency of the excited wave is close to the matching value, and the degree of mismatching of frequencies is likely to depend on the combined effect of both the wavenumber and frequency deviations from their matches that should benefit the energy exchange to the greatest extent. The matching relationships in the nonresonant interactions differ from the prediction in weak interaction theory. The nonresonant interaction has an irreversible excitation feature that for a nonresonant triad, if the excited wave substitutes any of the two initial waves, the anew excited wave is different from the substituted wave. Because of the complexity, for specified initial waves, it is difficult to predict both the wavelength and frequency of the excited wave in the nonresonant interaction.

In observational studies on the nonlinear interaction of gravity waves, owing to the observational restriction, the resonant interaction is supported only by the satisfaction of the matching condition at a certain wavenumber or frequency according to the spectral analysis of a series of spatial or temporal data. However, according to our study of the matching relationships in resonant and nonresonant interactions, this evidence should be insufficient for the resonant interaction, especially in the realistic background atmosphere with wind shear, temperature gradient and various dissipations. Nevertheless, if assuming that the background atmosphere is horizontally stratified, for the resonant and nonresonant interactions with considerable energy transfer, not only do the horizontal wavenumbers generally tend to approximately obey the matching condition but also the frequencies of the three waves may also approach a match. The study of nonlinear interactions of gravity waves in the realistic atmosphere still requires great efforts in terms of the theory, modeling and observations.

The authors thank the anonymous reviewers for their comments on the manuscript. This work was supported by National Natural Science Foundation of China (Grant Nos. 41074110, 41174133 and 40825013), National Basic Research Program of China (Grant No. 2012CB825605), Ocean Public Welfare Scientific Research Project, State Oceanic Administration People's Republic of China (Grant No. 201005017), China Meteorological Administration (Grant No. GYHY201106011) and Fundamental Research Funds for the Central Universities.

1 Lindzen R S. Turbulence and stress owing gravity wave and tidal breakdown. J Geophys Res, 1981, 86: 9707–9714

2 Holton J R. The role of gravity wave induced drag and diffusion in the momentum budget of the mesosphere. J Atmos Sci, 1982, 39: 791–799

3 Xu J, Smith A K, Collins R L, et al. Signature of an overturning gravity wave in the mesospheric sodium layer: Comparison of a nonlinear photochemical-dynamical model and lidar observations. J Geophys Res, 2006, 111, doi: 10.1029/2005JD006749

4 Hu X, Zhang X, Zhang D. Effects of atmospheric gravity waves on the mesosphere and lower thermosphere circulations. Chin J Space Sci, 2005, 25: 111–117

5 Fovell R, Durran D R, Holton J R. Numerical simulations of convectively generated stratospheric gravity waves. J Atmos Sci, 1992, 49: 1427–1442

6 Alexander M J, Holton J R, Durran D R. The gravity wave response above deep convection in a squall line simulation. J Atmos Sci, 1995, 52: 22299–22309

7 Yue J, Vadas S L, She C Y, et al. Concentric gravity waves in the mesosphere generated by deep convective plumes in the lower atmosphere near Fort Collins, Colorado. J Geophys Res, 2009, 114, doi: 10.1029/2008JD011244

8 Vadas S L, Fritts D C, Alexander M J. Mechanism for the generation of secondary waves in wave breaking regions. J Atmos Sci, 2003, 60: 194–214

9 Vadas S L, Liu H L. Generation of large-scale gravity wave and neutral winds in the thermosphere from the dissipation of convectively generated gravity waves. J Geophys Res, 2009, 114, doi: 10.1029/2009JA014108

10 Fritts D C, Alexander M J. Gravity wave dynamics and effects in the middle atmosphere. Rev Geophys, 2003, 41, doi: 10.1029/2001RG000106

11 Vincent R A, Alexander M J. Gravity waves in the tropical and lower stratosphere: An observational study of seasonal and interannual variability. J Geophys Res, 2000, 105: 17971–17982

12 Bian J, Chen H, Lu D. Statistics of gravity waves in the lower stratosphere over Beijing based on high vertical resolution radiosonde. Sci China SerD-Earth Sci, 2005, 48: 1548–1558

13 Alexander M J, Teitelbaum H. Observation and analysis of a large amplitude mountain wave event over the Antarctic peninsula. J Geophys Res, 2007, 112, doi: 10.1029/2006JD008368

14 Zhang S D, Yi F. Latitudinal and seasonal variations of inertial gravity wave activity in the lower atmosphere over central China. J Geophys Res, 2007, 112, doi: 10.1029/2006JD007487

15 Hines C O. The saturation of gravity wave in the middle atmosphere. Part II: Development of Doppler-spread theory. J Atmos Sci, 1991, 48: 1360–1379

16 Weinstock J. Theoretical gravity wave spectra in the atmosphere: Strong and weak interactions. Radio Sci, 1985, 20: 1295–1300

17 Yeh K C, Liu C H. Evolution of atmospheric spectrum by processes of wave-wave interactions. Radio Sci, 1985, 20: 1279–1294

18 Smith S A, Fritts D C, VanZandt T E. Evidence for a saturated spectrum of atmospheric gravity waves. J Atmos Sci, 1987, 44: 1404–1410

19 Yeh K C, Liu C H. The instability of atmospheric gravity waves through wave-wave interactions. J Geophys Res, 1981, 86: 9722–9728

20 Dong B, Yeh K C. Resonant and nonresonant wave–wave interactions in an isothermal atmosphere. J Geophys Res, 1988, 93: 3729–3744

21 Klostermeyer J. Two- and three-dimensional parametric instabilities in finite amplitude internal gravity waves. Geophys Astrophys Fluid Dyn, 1991, 64: 1–25

22 Fritts D C, Sun S J, Wang D Y. Wave-wave interactions in compressible atmosphere: 1. A general formulation including rotation and wind shear. J Geophys Res, 1992, 97: 9975–9988

23 Yi F, Xiao Z. Evolution of gravity waves through Resonant and nonresonant interactions in a dissipative atmosphere. J Atmos Sol-Terr Phys, 1997, 59: 305–317

24 Xiong J G, Yi F, Li J. The nonlinear interaction between Rossby wave and inertial gravity wave in the middle atmosphere, (1) The equations of nonlinear interaction. Chin J Geophys, 1995, 38: 150–157

25 Xiong J G, Yi F. Nonlinear interaction among planetary wave and inertial gravity wave in the middle and upper atmosphere. Chin J Space Sci, 2000, 20: 121–128

26 Müller P, Holloway G, Henyey F, et al. Nonlinear interactions among internal gravity waves. Rev Geophys, 1986, 24: 493–536

27 Dunkerton T J. Effect of nonlinear instability on gravity-wave momentum transport. J Atmos Sci, 1987, 44: 3188–3209

28 Vanneste J. The instability of internal gravity waves to localized disturbances. Ann Geophys, 1995, 13: 196–210

29 Yi F. Resonant interactions between propagating gravity wave packets. J Atmos Sol-Terr Phys, 1999, 61: 675–691

30 Zhang S D, Yi F. A numerical study on the propagation and evolution of resonant interacting gravity waves. J Geophys Res, 2004, 109, doi: 10.1029/2004JD004822

31 Huang K M, Zhang S D, Yi F. A numerical study on nonresonant interactions of gravity waves in a compressible atmosphere. J Geophys Res, 2007, 112, doi: 10.1029/2006JD007373

32 Huang K M, Zhang S D, Yi F. Gravity wave excitation through resonant interaction in a compressible atmosphere. Geophys Res Lett, 2009, 36, doi: 10.1029/2008GL035575

33 Huang K M, Zhang S D, Yi F. Propagation and reflection of gravity waves in a meridionally sheared wind field. J Geophys Res, 2008, 113, doi: 10.1029/2007JD008877

34 Hu Y Q, Wu S T. A full-implicit-continuous-Eulerian (FICE) multi-dimensional transient magnetohydrodynamic (MHD) flows. J Comput Phys, 1984, 55: 33–64

35 Tsuda T, Kato S, Yokoi T, Inoue T, et al. Gravity waves in the mesosphere observed with the middle and upper atmosphere radar. Radio Sci, 1990, 25: 1005–1018

36 Huang K M, Zhang S D, Yi F. Reflection and transmission of atmospheric gravity waves in a stably sheared horizontal wind field. J Geophys Res, 2010, 115, doi: 10.1029/2009JD012687